Design of Distributed Cooperative Control for Multi-Missile System to Track Maneuvering Targets

Belkacem Kada*, Khalid A. Juhany, Ibraheem Al-Qadi, Mostefa Bourchak
Aerospace Engineering Department, King Abdulaziz University, Jeddah, KSA

***Abstract*—The current paper provides unique smooth control methods for constructing resilient nonlinear autopilot systems and cooperative control protocols for single and multi-missile systems. To develop the single autopilots, a high-order framework based on asymptotic output stability principles and local relative degree for nonlinear affine systems is first applied. Then, using asymptotic exponential functions and graph theory, free-chattering distributed protocols are constructed to allow multi-missile systems to track and intercept high-risk targets. The Lyapunov approach is used to derive the essential requirements for smooth asymptotic consensus. The proposed method minimizes computing load while enhancing accuracy. The simulation results indicate the efficacy of the recommended strategies.**

***Keywords*—Multi-missile cooperative control; missile autopilot; smooth control; high-order sliding mode; target tracking**

I. INTRODUCTION

To adhere to the intended trajectory, a modern tactical missile (TM) autopilot system must be able to stabilize the rotational dynamics of the missile and accurately monitor the sequence of acceleration commands issued by the navigation and guidance system. However, constructing a missile's autopilot is a difficult challenge due to the unpredictability in aerodynamic derivatives.

Early missile autopilots were built using traditional methods, notably linearized dynamic models within a gain scheduling control approach. Using linear design methodologies within a gain scheduling framework, on the other hand, frequently resulted in suboptimal control where no stability or performance certificate could be given by the closed-loop system constituted of the nonlinear plant and planned controller. Several nonlinear control strategies have been developed to reduce the needed gain scheduling.

A nonlinear pitch-axis autopilot involving scheduling linear H_∞ control design under constant operating conditions and bounded scheduling variables was first discussed in [1]. In the work presented in [2], gain-scheduling and gap metric techniques were used to design a robust missile pitch-axis autopilot for an air-to-air missile. The connection between the loop-shaping theory and the gap metric technique was used to compute the operating points, and proportional-integral/proportional-type controllers were designed. The problem of the missile's autopilot design in the presence of hidden coupling terms was tackled in [3] using gain-scheduling control. The study introduced a self-scheduling method for preserving the local properties of the nonlinear gain-scheduled controller, which allows for consideration of the hidden coupling terms during the design process. The nonlinear pitch dynamics of a tail-controlled, extremely agile missile were addressed in [4] by designing a gain-scheduled 4-loop autopilot. The requirements for an autopilot's design were methodically converted into hard and soft tuning objectives, and the resulting multi-model/multi-objective issue was then addressed with the help of a nonsmoothed optimization process.

Many design schemes have recently been developed to provide stringent performance requirements and ensure robustness across different flight conditions. The Linear Parameter Varying (LPV) approach was recently used conjointly with linear fractional transformation (LFT) in [5] to design specified structure autopilots that ensure robustness to a large class of uncertainty. The proposed LPV/LFT algorithm could handle slope-restricted nonlinearities and rate-bounded time-varying parameters using a nonsmooth optimization technique and using polytopic LPV weights within the four-block loop-shaping H∞ loop shaping theory, the authors, in [6], designed an output feedback controller to provide a missile longitudinal autopilot with robust H∞ performance. To accommodate the seeker field-of-view constraint while maintaining the system's resilience, an integrated missile guidance and control method was developed in [7] by appending the integral barrier Lyapunov function to dynamic surface control. As uncertain disturbances of the system, the authors treated target maneuvering and unmodeled disturbances with the influence of the disturbance rejection rate error. They employed an extended state observer for real-time estimates.

The study in [8] offered a sliding mode control (SMC) architecture for precision missile operation inside a nonlinear finite-time control framework, as opposed to the asymptotically convergent control framework. The study's most significant contribution was analysing the influence of boundary layer thickness on missile system reactions, with the assumption that reducing boundary layer thickness will improve the control performance of the SMC autopilot system.

On the other hand, as the multilayered missile defense system has been refined and target maneuverability has increased, the challenge of penetrating a target with a single traditional missile has increased in recent years. In such a case, cooperative guiding is recommended as a viable countermeasure to boost missile penetrability. To improve the lethality of multiple missiles, cooperative guiding laws must also meet time and space restrictions, in addition to attaining a minimal or even zero miss distance. Many recent studies [9-

14] have concentrated on the topic of distributed cooperative guidance of multi-missile systems.

In this study, we first suggested a new high-order SMC-based technique for developing the guidance law, which serves as the foundation for estimating the ideal flying AOA and normal acceleration trajectories. The goal of this technique is to look at the use of finite-time control for the longitudinal dynamics of a tactical missile, with the needed information acting as the control command. We propose a smooth control-based design of distributed consensus protocols for multi-missile system guiding in the second half. Free-chattering distributed protocols are constructed using asymptotic exponential functions and graph theory. The essential criteria for smooth asymptotic tracking are derived using the Lyapunov method.

II. Missile Dynamics and Control Objectives

A TC system is a type of guided missile designed for use in combat situations with a relatively limited range, typically within the theatre of operations or on the battlefield. These missiles are designed to execute pinpoint attacks against hostile installations, vehicles, aircraft, and ships. Fig. 1 shows a typical TM model.

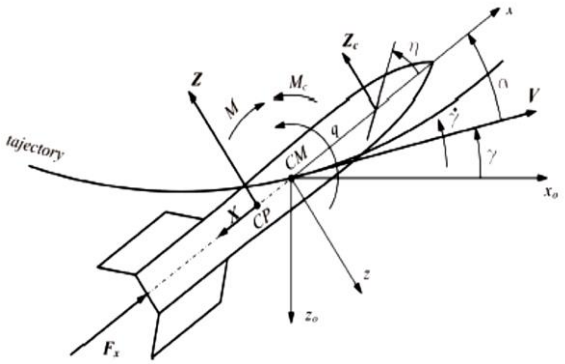

Fig. 1. Missile pitch-axis motion.

The Reichert's missile model [1], a hypothetical fin-controlled pitch-axis missile that serves as a standard in studies of nonlinear controller design for supersonic and hypersonic vehicles, is employed as the basis for the present study.

The nonlinear dynamic model presented below governs the missile's motion in the planar space.

$$\dot{M} = K_z M^2 \left[C_{D_0} - C_z(\alpha, M) sin\alpha\right] - \frac{g}{v_s} sin\gamma \quad (1)$$

$$\dot{\alpha} = K_z M C_z(\alpha, M) co\frac{g}{v_s M} cos\gamma + q \quad (2)$$

$$\dot{q} = K_m M^2 C_m(\alpha, M) \quad (3)$$

$$\dot{\gamma} = -K_z M C_z(\alpha, M) cos\alpha - \frac{g}{v_s M} cos\gamma \quad (4)$$

where:

- M is the Mach number.
- α is the angle-of-attack (AOA) (rad).
- q is the pitch rate (rad/s).
- γ is the flight path angle (rad).

The nonlinear coefficients C_z and C_m characterize the missile aerodynamics model's and are given as time-varying parameters.

$$C_z = a_z\alpha^3 + b_z|\alpha|\alpha + c_z\left(2 - {}^{M}/_{3}\right)\alpha + d_z\delta \quad (5)$$

$$C_m = a_m\alpha^3 + b_m|\alpha|\alpha + c_m\left(-7 + {}^{8M}/_{3}\right) + e_m q + d_m\delta \quad (6)$$

Considering the above four flight parameters as system's states and the fin deflection (6) as control input, model (1)-(4) becomes.

$$\begin{aligned} \dot{\boldsymbol{x}} &= \boldsymbol{f}(\boldsymbol{x}) + \boldsymbol{g}(\boldsymbol{x})u \\ y &= h(\boldsymbol{x}) \end{aligned} \quad (7)$$

with

$$\boldsymbol{x} = [M\ \alpha\ q\ \gamma]^T \quad (8)$$

$$h = \eta(M, \alpha) \quad (9)$$

$$u = \delta \quad (10)$$

where the missile's normal acceleration η is given by

$$\eta = K_z M^2 v_s C_z(\alpha, M) \quad (11)$$

and $\boldsymbol{f}(\boldsymbol{x}) \in \mathbb{R}^4$, $\boldsymbol{g}(\boldsymbol{x}) \in \mathbb{R}^4$, and $h(\boldsymbol{x}) = \eta \in \mathbb{R}$ are uncertain bounded functions. $\boldsymbol{f}(\boldsymbol{x}), \boldsymbol{g}(\boldsymbol{x})$ and $h(\boldsymbol{x})$ are uncertain due the uncertainty of the aerodynamics coefficients given in (5) and (6). The expended form of the model (7) is given below:

$$\begin{aligned} f_1(\boldsymbol{x}) = -\frac{g}{v_s} sinx_3 - K_z x_1^2 \big[C_{D_0} - \\ \left(a_z x_2^3 + b_z|x_2|x_2 + c_z\left(2 - {}^{x_1}/_{3}\right)x_2\right)\big] sinx_2 \end{aligned} \quad (12)$$

$$\begin{aligned} f_2(\boldsymbol{x}) = +\frac{g}{v_s x_1} cosx_3 + x_4 K_z x_1 [a_z x_2^3 + b_z|x_2|x_2 \\ + c_z\left(2 - {}^{x_1}/_{3}\right)x_2]\, cosx_2 \end{aligned} \quad (13)$$

$$\begin{aligned} f_3(\boldsymbol{x}) = -K_z x_1 [a_z x_2^3 + b_z|x_2|x_2 - \frac{g}{v_s x_1} cosx_3 \\ + \left(2 - {}^{x_1}/_{3}\right)x_2]\, cosx_2 \end{aligned} \quad (14)$$

$$f_4(\boldsymbol{x}) = K_m x_1^2 [a_m x_2^3 + b_m|x_2|x_2 \left(-7 - {}^{8x_1}/_{3}\right) x_2] \quad (15)$$

$$\boldsymbol{g}(\boldsymbol{x}) = [0\ \ 0\ \ 0\ \ K_m x_1^2 d_m]^T \quad (16)$$

$$\begin{aligned} h(\boldsymbol{x}) = K_z x_1 [a_z x_2^3 + b_z|x_2|x_2 \\ + c_z\left(2 - {}^{x_1}/_{3}\right)x_2]. \end{aligned} \quad (17)$$

Achieving the intended mission in a short time while accounting for external disturbances and model uncertainties is the goal of the present control design. The performance objectives for the closed-loop system encompass the achievement of finite-time closed-loop convergence, fast response to substantial manoeuvres, the system's ability to withstand and adapt to plant uncertainties and disturbances.

III. High-Order Sliding Mode Control to Missile Autopilot Design

A. Lie Derivatives for Nonlinear Affine Control

Consider a vector field $f(x) \in \mathbb{R}^n$ defined on open operating domain $D \in \mathbb{R}^n$ and a smooth map $m \in \mathbb{R}^p$. For any $x \in m$, The Lie derivatives, along the trajectory $f(x)$, for the map m are given as follows:

$$L_f m(x) = \frac{d}{dt} m\left(\phi_i^f(x)\right)\Big|_{t=0} \tag{18}$$

where, $\phi_i^f(x)$ denotes the flow vector of $f(x)$ at time t. Using the chain rule, one can write

$$L_f m(x) = m^{(1)}(x) f(x) \tag{19}$$

with $m^{(1)} = \partial m / \partial x$ being the Jacobian matrix of m. Therefore, the *r*-derivative of m is given as

$$\begin{cases} L_f^r m(x) = m^{(r-1)}(x) f(x) \\ L_f^0 m(x) = m(x) \end{cases} \tag{20}$$

According to the Lie derivatives properties, for a further vector g, expression (20) becomes

$$L_g L_f m(x) = \frac{\partial L_f m(x)}{\partial x} g(x) \tag{21}$$

B. Sliding Mode Control Design

Consider the following tracking error to be the actual output of a multi-output system with $\in \mathbb{R}^p$.

$$e(y) = y - y_d \tag{22}$$

where, y_d denotes the desired values of y. The system equilibrium point is located on the manifold $e_i^{-1}(0)) = \{x | \, e_i(x) = 0\}$).

Definition 1. The derivative degree r in equation (20) extends, for the case (22), to the vector $r = \left[r_1 \, r_2 \, \ldots \, r_p\right]^T$ for which expression (20) and (21), for a given initial condition x_0, become

$$\begin{cases} L_g L_f^k e_i(x) = 0 \\ L_g L_f^{r_i - 1} e_i(x_0) \neq 0 \end{cases} \quad 0 \leq k \leq r_i - 2, 1 \leq i \leq p \tag{23}$$

Following is the calculation of the derivatives in (23) that appear in sequence.

$$\begin{bmatrix} L_f \\ L_f^k \\ L_g \end{bmatrix} e_i(x) = \begin{bmatrix} \sum_{i=1}^n \frac{\partial e_i}{\partial x_i} f_i(x) \\ L_f\left(L_f^{k-1} e_i(x)\right) \\ \sum_{i=1}^n \frac{\partial e_i}{\partial x_i} g_i(x) \end{bmatrix} \tag{24}$$

Lemma 1 [xx]. If and only if the following holds for any subset of the domain of the output e_i, then the relative degree r_i is well-defined there.

$$L_g L_f^{r_i - 1} e_i(x_0) = \tau \tag{25}$$

where τ is a constant.

Lemma 2 [xx]. For each e_i with $r_i > 1$, a stable motion towards zero can be obtained for the sequence $\left(e_i, e_i^{(1)}, e_i^{(2)}, \ldots, e_i^{(r_i - 1)}\right)$ by designing the following sliding manifold that satisfies $\sigma_i^{-1}(0) = \{x | \, \sigma_i(x) = 0\}$

$$\begin{aligned} \sigma_i(x) = \; & L_f^{r_i - 1} e_i(x) + \lambda_{r_i - 2} L_f^{r_i - 2} e_i(x) + \cdots \\ & + \lambda_1 L_f e_i(x) + \lambda_0 e_i(x) \, . \end{aligned} \tag{26}$$

with $\lambda_j > 0$ ($j = r_i - 2, \ldots, 0$) define design parameters.

Lemma 3 [xx]: The following equation has a single local solution, denoted by the affine control u(x)

$$\begin{aligned} & \left[L_f \sigma_i(x)\right] = \Big[L_f^{r_i} e_i(x) + \\ & \lambda_{r_i - 2} L_f^{r_i - 1} e_i(x) + \cdots + \lambda_0 L_f e_i(x)\Big] = 0 \end{aligned} \tag{27}$$

Remark 1: If a relative degree r_i is defined for each output y_i with respect to a control input u, then the smallest relative degree $\rho > 1$ is considered as the relative degree of the whole system (i.e., $\rho = \min(r_i)$, and $\rho > 1$).

Remark 2: A well-defined relative degree guarantees the applicability of such a controller over the working range, while the smallest relative degree simplifies the design task and gives a practical controller. The outer-loop sliding mode controller's primary characteristic is shown in the following block diagram.

C. AOA Autopilot

With $e_2 = \alpha - \alpha_d = x_2 - x_{2,d}$ and $\frac{\partial \alpha_d}{\partial x} = \frac{\partial x_{2,d}}{\partial x}$, the Lie derivatives (24) are computed as follows

$$L_g \begin{bmatrix} e_1(x) \\ e_2(x) \\ e_3(x) \end{bmatrix} = L_g L_f \begin{bmatrix} e_1(x) \\ 0 \\ e_3(x) \end{bmatrix} = 0_{3x1} \tag{28}$$

$$L_g L_f^2 \begin{bmatrix} e_1(x) \\ e_2(x) \\ e_3(x) \end{bmatrix} = g(x) \begin{bmatrix} \frac{\partial f_1(x)}{\partial x_2} \\ 1 \\ \frac{\partial f_3(x)}{\partial x_2} \end{bmatrix} \tag{29}$$

Considering property (25), the AOA's relative degree is $r_\alpha = 2$. This proves that there exists a well-defined output-input assignment $\forall x \in \mathrm{O}(x_0)$. According to the value of r_α, the sliding manifold (26) becomes

$$\sigma(x) = \frac{\partial e_2}{\partial x} f \; + \lambda e_2 = \frac{\partial x_2}{\partial x} f \; + \lambda\left(x_2 - x_{2,d}\right) \tag{30}$$

Applying Lemma 3, the fin deflection that ensure $\sigma(x) = 0$ is derived as follows:

$$\delta(x) = \left(\frac{1}{1 + g(x)}\right) - \left(u(x) + K sat\left(\sigma(x)/\varepsilon\right)\right) \tag{31}$$

where the saturation function is implemented using a boundary layer ε s

$$sat(^{\sigma}/_{\varepsilon}) = \begin{cases} ^{\sigma}/_{\varepsilon} & if\ |^{\sigma}/_{\varepsilon}| \le 1 \\ sgn(^{\sigma}/_{\varepsilon}) & if\ |^{\sigma}/_{\varepsilon}| > 1 \end{cases} \quad (32)$$

In this design, the gain K is provided to correct model uncertainties, unmodeled dynamics, and measurement noises, the coefficient sets the bandwidth of the error dynamics, and the layer ε is introduced to dampen the babbling.

D. Normal Acceleration Autopilot

The rate of the missile's acceleration is one of the primary variables managed by an autopilot system. Commonly symbolized by the letter "g" normal acceleration quantifies the gravitational pull experienced by the airframe in flight. Using normal acceleration autopilot to deflect the fins allows controlling a measured variable, which avoids the use of an estimator for α. To do so, we compute the inverse transformation of Eq. (11).

$$\alpha(\eta, M) = K_z M^2 \begin{bmatrix} \dfrac{2b_z^2 - a_z c_z\left(2 - {}^{M}/_{3}\right)}{K_z^3 M^2 c_z^5 \left(2 - {}^{M}/_{3}\right)^5} \eta^3 \\ - \dfrac{b_z}{K_z^2 c_z^3 \left(2 - {}^{M}/_{3}\right)^3} |\eta|\eta \\ + \dfrac{1}{K_z M^2 c_z \left(2 - {}^{M}/_{3}\right)} \eta \end{bmatrix} \quad (33)$$

From (33), the time derivative of η is given as follows

$$\dot{\eta} = \left(\frac{\partial \alpha}{\partial \eta}\right)^{-1} \left[K_z M C_z(M, \eta) + q(M, \eta) - \frac{\partial P}{\partial M} \dot{M}(M, \eta)\right] \quad (34)$$

The sliding manifold and its corresponding control input are given as follows

$$\begin{cases} \sigma(x) = \frac{\partial \eta}{\partial x} f \ \ + \lambda(\eta - \eta_d) \\ \frac{\partial}{\partial \gamma} \frac{\partial \dot{\eta}}{\partial x} f(x) + \lambda \frac{\partial \dot{\eta}}{\partial \gamma} = 0 \end{cases} \quad (35)$$

IV. Distributed Missile Autopilot Design

In the context of a fixed topology, we present, in this section, the design of distributed consensus protocols u_i to allow a multi-missile system, composed of m agents, to track an AOA or normal acceleration commands to ensure a successful interception of high-risk targets. To do so, a consensus tracking error is defined as follows:

$$e_i = \sum_{j=0}^{n} a_{ij}\left(x_i(t) - x_j(t)\right) \quad (36)$$

where, a_{ij} denote the elements of the the adjacent matrix $\mathcal{A}$ and $x_i \in \mathbb{R}^n$ denotes the individual missiles state vector.

Definition 2: Based on the consensus (36), we define, for each agent 'i' (e.g., individual missile) the following inequality.

$$\|\psi_i(e_i)\|_2 \le \|\psi_i(e_i)\|_1 \le N\|\psi_i(e_i)\|_\infty \le N\kappa \quad (37)$$

with $N = nm$ and $\kappa \in \mathbb{R}^+$

Definition 3: According to the communication graph $\mathcal{G}$ of the multi-missile system, we define a matrix M such that $M = \mathcal{L} + \mathcal{D}_0$ with $\mathcal{L} = \mathcal{D} - \mathcal{A}$ being the Laplacian matrix associated with $\mathcal{G}$, $\mathcal{D}_0 = diag(a_{i0})$, and $\mathcal{D} = diag(d_i = \sum_{j=1}^{n} a_{ij})$.

Definition 4: The missiles' dynamics are bounded

$$\|f_i(x_i)\|_2 \le \rho\|x_i\|_2, \|f_i(x) - f_i(y)\|_2 \le \gamma\|x - y\|_2 \quad (38)$$

with $\rho, \gamma \in \mathbb{R}^+$.

Theorem 1: Based on the properties of the matrix M, If the fixed-time undirected graph $\mathcal{G}$ is connected and at least one $a_{i0} > 0$, the leader-follower consensus (36) is asymptotically guaranteed by the following distributed consensus control.

$$u_i = -k_1 e_i - k_2 \psi_i(e_i) \quad (39)$$

where, k_1, k_2 are the consensus gains satisfying.

$$\begin{cases} k_1 \ge \rho \dfrac{\lambda_{\max}(\boldsymbol{M})}{\lambda_{\min}^2(\boldsymbol{M})} \\ k_2 \ge \dfrac{\sqrt{\tilde{\boldsymbol{x}}_0^T(\boldsymbol{M} \otimes \boldsymbol{I}_N)\tilde{\boldsymbol{x}}_0}\sqrt{\lambda_{\max}(\boldsymbol{M})}}{t_s \lambda_{\min}(\boldsymbol{M}) N\kappa}(1 + d_0) \\ t_s = \dfrac{\sqrt{\tilde{\boldsymbol{x}}_0^T(\boldsymbol{M} \otimes \boldsymbol{I}_N)\tilde{\boldsymbol{x}}_0}\sqrt{\lambda_{\max}(\boldsymbol{M})}}{k_2 \lambda_{\min}(\boldsymbol{M}) N\kappa} \end{cases} \quad (40)$$

with $\lambda_{min}(M) > 0$, $\kappa > 0$, and t_s is the settling time.

Proof:

For each agent 'i', let us consider a tracking error denoted as $\tilde{x}_i = x_i - x_0$. By employing the distributed consensus protocol (38), the multi-agent closed-loop system is written as follows:

$$\dot{\tilde{x}}_i = f_i(x_i) - f_0(x_0) - k_1 \sum_{j=1}^{n} a_{ij}\left(\tilde{x}_i - \tilde{x}_j\right) - k_2 \psi_i(\tilde{e}_i) \quad (41)$$

where, $\tilde{e}_i = \sum_{j=0}^{n} a_{ij}\left(\tilde{x}_i - \tilde{x}_j\right)$. For the muti-agent system, we write

$$\dot{\tilde{x}} = F(\tilde{x}, \tilde{x}_0) - k_1(M \otimes I_N)\tilde{x} - k_2 \Psi(\tilde{e}) \quad (42)$$

with

$$\tilde{x} = [\tilde{x}_1^T, \dots, \tilde{x}_n^T]^T,$$
$$F(\tilde{x}, x_0) = \left[\left(f_1(x_1) - f_0(x_0)\right)^T, \dots \left(f_n(x_n) - f_0(x_0)\right)^T\right]^T,$$
$$\Psi(\tilde{e}) = [\psi_1^T(\tilde{e}_1), \dots, \psi_n^T(\tilde{e}_n)]^T$$

where, $f_0(x_0)$ denotes the vector field of the leader dynamics and x_0 denotes its state vector. To demonstrate the effectiveness of the proposed control algorithm, we consider the following Lyapunov function candidate.

$$V = \frac{1}{2}\tilde{x}^T(M \otimes I_N)\tilde{x} \quad (43)$$

for which,

$$\dot{V} = \tilde{x}^T(M \otimes I_N)[F(\tilde{x}, x_0) - k_1(M \otimes I_N)\tilde{x} - k_2\Psi(\tilde{e})] \quad (44)$$

with $\lambda_{min}(M) > 0$, one can get

$$\begin{cases} \tilde{x}^T(M \otimes I_N)F((\tilde{x}, x_0)) = F^T((\tilde{x}, x_0))(M \otimes I_N)\tilde{x} \\ \qquad \leq \rho\lambda_{max}(M)\|\tilde{x}\|_2^2 \\ \tilde{x}^T(M \otimes I_N)^2\tilde{x}\,\lambda_{min}^2 \quad (M)\|\tilde{x}\|_2^2 \end{cases} \quad (45)$$

It results,

$$\dot{V} \leq -k_1\lambda_{min}^2(M)\|\tilde{x}\|_2^2 - \rho\lambda_{max}(M)\|\tilde{x}\|_2^2 + \lambda_{min}(M)\|\Psi(\tilde{e})\|_2\|\tilde{x}\|_2 \quad (46)$$

Suppose that there exist $\kappa \in \mathbb{R}^+$ for which

$$\|\psi_i(e_i)\|_2 \leq \|\psi_i(e_i)\|_1 \leq N\|\psi_i(e_i)\|_\infty \leq N\kappa \quad (47)$$

It results that condition (46) is achieved if and only if

$$k_1\lambda_{min}^2(\boldsymbol{M})\|\tilde{\boldsymbol{x}}\|_2^2 - \rho\lambda_{max}(\boldsymbol{M})\|\tilde{\boldsymbol{x}}\|_2^2 = \left(k_1 - \rho\frac{\lambda_{max}(\boldsymbol{M})}{\lambda_{min}^2(\boldsymbol{M})}\right)\lambda_{min}^2(\boldsymbol{M})\|\tilde{\boldsymbol{x}}\|_2^2 \geq 0$$

$$k_2\lambda_{min}(\boldsymbol{M})\|\boldsymbol{\Psi}(\tilde{\boldsymbol{e}})\|_2\|\tilde{\boldsymbol{x}}\|_2 - d_0 = \frac{k_2\lambda_{min}(\boldsymbol{M})\sqrt{2V}}{\sqrt{\lambda_{max}(\boldsymbol{M})}}\|\boldsymbol{\Psi}(\tilde{\boldsymbol{e}})\|_2 - d_0 \geq 0 \quad (48)$$

where, d_0 is the maximum value of an eventual disturbance ($d_0 = 0$ for undisturbed system). With $k_1 \geq \rho\frac{\lambda_{\max}(M)}{\lambda_{min}^2(M)}$, $\dot{V}$ will satisfy

$$\dot{V} \leq -\frac{k_2\lambda(M)\sqrt{2V}_{min}}{\sqrt{\lambda(M)_{max}}\|\Psi(\tilde{e})\|_1} \leq -\frac{k_2\lambda(M)\sqrt{2V}_{min}}{\sqrt{\lambda(M)_{max}}N\|\Psi(\tilde{e})\|_\infty} \quad (49)$$

It follows,

$$\begin{cases} \sqrt{V} \leq \sqrt{V_0} - \frac{k_2}{\sqrt{2}}\frac{\lambda(M)\|\Psi(\tilde{e})\|_{\infty min}}{\sqrt{\lambda(M)_{max}}t} \\ t_s = \frac{\sqrt{\tilde{x}_0^T(M\otimes I_N)\tilde{x}_0}\sqrt{\lambda(M)_{max}}}{k_2\lambda(M)_{min}} \\ k_1 \geq \rho\frac{\lambda_{max}}{\lambda_{min}^{2(M)}} \\ k_2 \geq \frac{\sqrt{\tilde{x}_0^T(M\otimes I_N)\tilde{x}_0}\sqrt{\lambda(M)_{max}}}{t_s\lambda(M)_{min}(1+d_0)} \end{cases} \quad (50)$$

V. Results and Discussion

First scenario: A quick, high-maneuver normal acceleration tracking scenario is used to assess the performance and reliability of the normal acceleration autopilot for a single missile airframe. As it can be seen in Fig. 2, the commanded acceleration and initial Mach number were chosen at their extremes. The results show that the proposed technique is effective for controlling such complex system.

Second scenario: In this section, first, the tracking of an AOA sequence using the state feedback-based autopilot is performed by a multi-missile composed of six agents. The AOA sequence is introduced as step commands given at different initial AOA $\alpha_0 = [-5 \quad 0 \quad 20 \quad -7.5 \quad 5 \quad -20]^T$ and $M = 3$. The communication topology is shown in Fig. 3 and the time-history of the tracking mission is shown in Fig. 4.

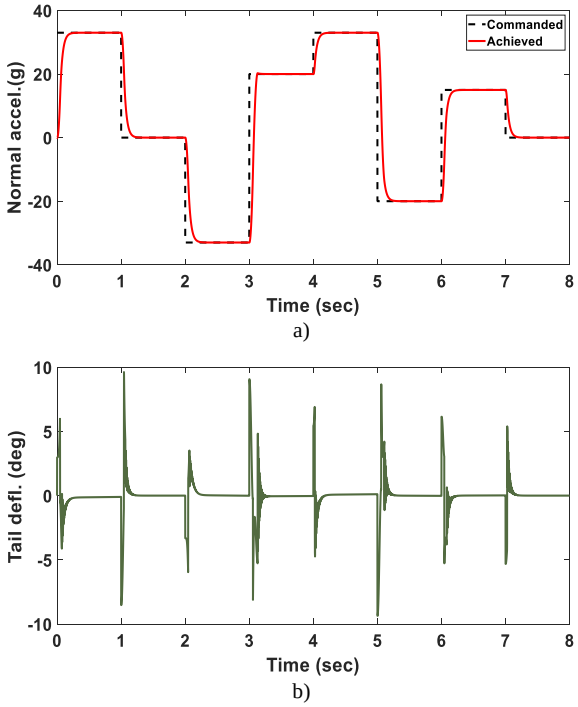

Fig. 2. Single missile response to a normal acceleration pattern: a) Normal acceleration, b) Tail deflection.

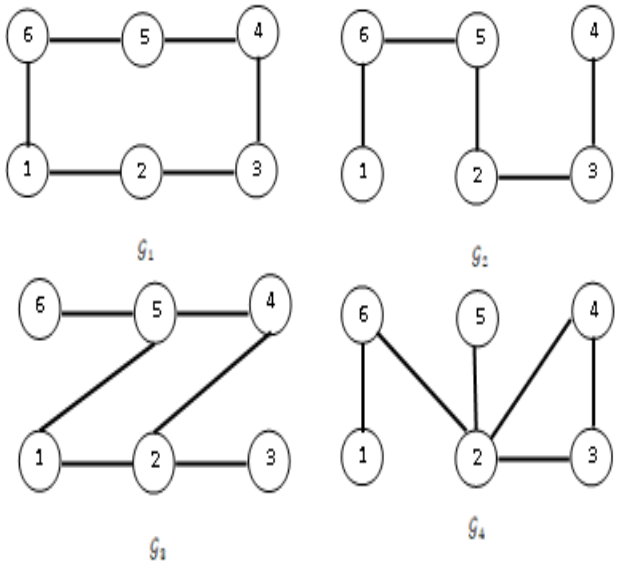

Fig. 3. Fixed-time switching topology connected interaction graph.

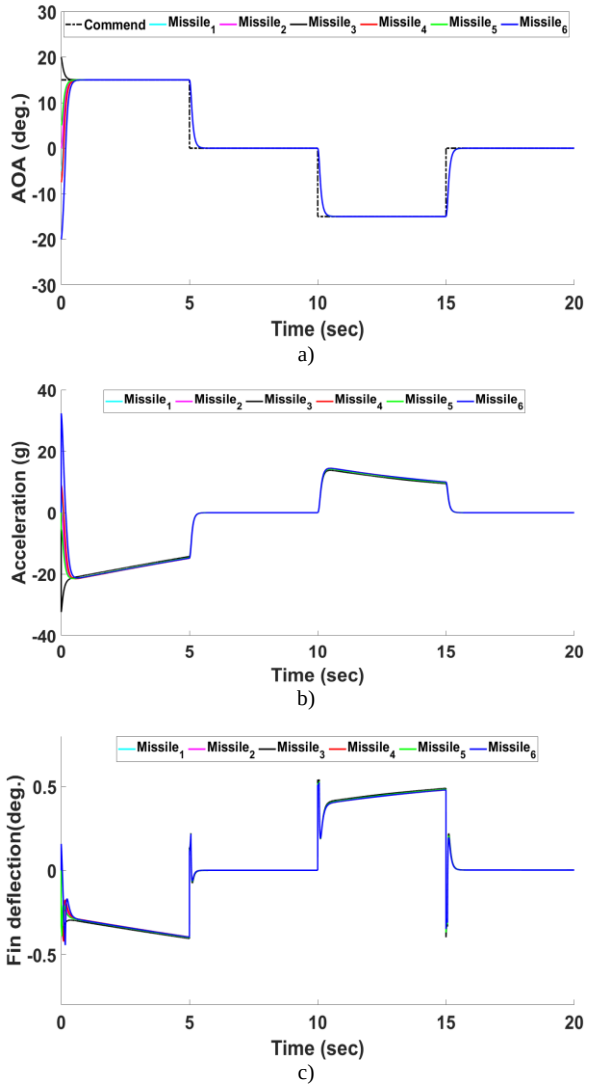

Fig. 4. Time history of multi-missile system response: a) AOA, b) Normal acceleration, C) Fin deflection.

VI. CONCLUSION

In this study, we first designed two robust longitudinal autopilot topologies for a tail-controlled tactical missile. The two autopilots were created with high-order sliding mode control and a thorough nonlinear dynamic model. Second, we looked at the distributed control-based cooperative guiding problem for a multi-missile system intercepting a high-risk target. Asymptotic exponential functions and graph theory were used to create free-chattering distributed protocols. The Lyapunov technique was used to determine the necessary requirements for smooth asymptotic tracking. The simulation findings show that there is reduced computing load and more precision. Future study will focus on various features of multi-missile systems for practical implementations, such as the distinct overload and impact angle limits of each missile, communication delays, and robustness consensus.

ACKNOWLEDGMENT

This project was funded by the Deanship of Scientific Research (DSR), King Abdulaziz University, Jeddah, under grant No. (G-1454-135-1440). The authors, therefore, gratefully acknowledge DSR technical and financial support.

REFERENCES

[1] Nichols A. Robert, Reichert T, Robert, and Rugh J. (1993). Gain Scheduling for H-Infinity Controllers: A Flight Control Example. In: IEEE Transactions on Control Systems Technology. vol. 1, No. 2, pp 69-79.

[2] Theodoulis S. and Duc G., "Missile Autopilot Design: Gain-Scheduling and the Gap Metric," Journal of Guidance, Control, and Dynamics, Vol. 32, No. 3, 2009, pp. 986–996.

[3] Lhachemi H., Saussié D. and Zhu G., "Gain-Scheduling Control Design in the Presence of Hidden Coupling Terms," Journal of Guidance, Control, and Dynamics, Vol. 39, No. 8, 2016, pp. 1871–1879.

[4] heodoulis S., Proff M. and Marchand C., "Robust Design for Highly Agile Missile Autopilots," 28th Mediterranean Conference on Control and Automation, Inst. of Electrical and Electronics Engineers, New York, 2020, pp. 67–72.

[5] Alberto M. Simões and Vinícius M. G. B. Cavalcanti (2023). Missile Autopilot Design via Structured Robust Linear Parameter-Varying Synthesis, Journal of Guidance, Contrand Dynamics, vol. 46, no. 8, doi:10.2514/1.g007580.

[6] Y. M. Tavares and J. Waldmann, "H∞ Loop Shaping Using Polytopic Weights and Pole Assignment to Missile Autopilot," in *IEEE Access*, vol. 11, pp. 125-133, 2023, doi: 10.1109/ACCESS.2022.3232464.

[7] S. -Y. Lin, J. Wang and W. Wang, "Barrier Lyapunov Function Based Integrated Missile Guidance and Control Considering Phased Array Seeker Disturbance Rejection Rate," in *IEEE Access*, vol. 10, pp. 31070-31083, 2022, doi: 10.1109/ACCESS.2022.3156292.

[8] Yadong, C., Zhaoke, N., Kai, Z., Bin, L. (2023). Multi-missile Cooperative Strike on Stationary Target Based on Distributed Model Predictive Control. In: Yan, L., Duan, H., Deng, Y. (eds) Advances in Guidance, Navigation and Control. ICGNC 2022. Lecture Notes in Electrical Engineering, vol 845. Springer, Singapore. https://doi.org/10.1007/978-981-19-6613-2_261.

[9] W. Tian, Q. Yang and Q. Zhao, "Cooperative Guidance of Multi-missile over Random Communication Networks," *2022 34th Chinese Control and Decision Conference (CCDC)*, Hefei, China, 2022, pp. 5602-5607, doi: 10.1109/CCDC55256.2022.10033769.

[10] Q. Wang, P. Lu and Y. Tian, "Finite-time Simultaneous-Arrival-To-Origin Sliding Model Control for Multi-missile Systems," *2023 42nd Chinese Control Conference (CCC)*, Tianjin, China, 2023, pp. 129-133, doi: 10.23919/CCC58697.2023.10240566.

[11] J. Zhou, X. Nan, S. Wang and D. Zhao, "Distributed guidance design for multi-missile sequential attacks," *2022 IEEE International Conference on Unmanned Systems (ICUS)*, Guangzhou, China, 2022, pp. 578-583, doi: 10.1109/ICUS55513.2022.9986858.

[12] Hou, Z., Lan, X., Chen, H. *et al.* Finite-time Cooperative Guidance Law for Multiple Missiles with Impact Angle Constraints and Switching Communication Topologies. *J Intell Robot Syst* **108**, 85 (2023). https://doi.org/10.1007/s10846-023-01931-1.

[13] Zhang, M., Ma, J., Che, R., He, Y. (2022). Fixed-Time Convergence Cooperative Guidance Law Against Maneuvering Target. In: Yan, L., Duan, H., Yu, X. (eds) Advances in Guidance, Navigation and Control. Lecture Notes in Electrical Engineering, vol 644. Springer, Singapore. https://doi.org/10.1007/978-981-15-8155-7_332.

[14] Zhongyuan Chen, Xiaoming Liu, Wanchun Chen, Three-dimensional event-triggered fixed-time cooperative guidance law against maneuvering target with the constraint of relative impact angles, Journal of the Franklin Institute, Volume 360, Issue 6, 2023, Pages 3914-3966. https://doi.org/10.1016/j.jfranklin.2023.02.027.